

PROCEEDINGS OF SPIE

SPIDigitalLibrary.org/conference-proceedings-of-spie

Concept design of the LiteBIRD satellite for CMB B-mode polarization

Y. Sekimoto, P. Ade, K. Arnold, J. Aumont, J. Austermann, et al.

Y. Sekimoto, P. Ade, K. Arnold, J. Aumont, J. Austermann, C. Baccigalupi, A. Banday, R. Banerji, S. Basak, S. Beckman, M. Bersanelli, J. Borrill, F. Boulanger, M. L. Brown, M. Bucher, E. Calabrese, A. Challinor, Y. Chinone, F. Columbro, A. Cukierman, D. Curtis, P. de Bernardis, M. de Petris, M. Dobbs, T. Dotani, L. Duband, A. Ducout, K. Ebisawa, T. Elleflot, H. Eriksen, J. Errard, R. Flauger, C. Franceschet, U. Fuskeland, K. Ganga, J.R. Gao, T. Ghigna, J. Grain, A. Gruppuso, N. Halverson, P. Hargrave, T. Hasebe, M. Hasegawa, M. Hattori, M. Hazumi, S. Henrot-Versille, C. Hill, Y. Hirota, E. Hivon, D. T. Hoang, J. Hubmayr, K. Ichiki, H. Imada, H. Ishino, G. Jaehnig, H. Kanai, S. Kashima, Y. Kataoka, N. Katayama, T. Kawasaki, R. Keskitalo, A. Kibayashi, T. Kikuchi, K. Kimura, T. Kisner, Y. Kobayashi, N. Kogiso, K. Kohri, E. Komatsu, K. Komatsu, K. Konishi, N. Krachmalnicoff, C. L. Kuo, N. Kurinsky, A. Kushino, L. Lamagna, A. T. Lee, E. Linder, B. Maffei, M. Maki, A. Mangilli, E. Martinez-Gonzalez, S. Masi, T. Matsumura, A. Mennella, Y. Minami, K. Mistuda, D. Molinari, L. Montier, G. Morgante, B. Mot, Y. Murata, A. Murphy, M. Nagai, R. Nagata, S. Nakamura, T. Namikawa, P. Natoli, T. Nishibori, H. Nishino, F. Noviello, C. O'Sullivan, H. Ochi, H. Ogawa, H. Ogawa, H. Ohsaki, I. Ohta, N. Okada, G. Patanchon, F. Piacentini, G. Pisano, G. Polenta, D. Poletti, G. Puglisi, C. Raun, S. Realini, M. Remazeilles, H. Sakurai, Y. Sakurai, G. Savini, B. Sherwin, K. Shinozaki, M. Shiraiishi, G. Signorelli, G. Smecher, R. Stompor, H. Sugai, S. Sugiyama, A. Suzuki, J. Suzuki, R. Takaku, H. Takakura, S. Takakura, E. Taylor, Y. Terao, K. L. Thompson, B. Thorne, M. Tomasi, H. Tomida, N. Trappe, M. Tristram, M. Tsuji, M. Tsujimoto, S. Uozumi, S. Utsunomiya, N. Vittorio, N. Watanabe, I. Wehus, B. Westbrook, B. Winter, R. Yamamoto, N. Y. Yamasaki, M. Yanagisawa, T. Yoshida, J. Yumoto, M. Zannoni, A. Zonca, "Concept design of the LiteBIRD satellite for CMB B-mode polarization," Proc. SPIE 10698, Space Telescopes and Instrumentation 2018: Optical, Infrared, and Millimeter Wave, 106981Y (9 August 2018); doi: 10.1117/12.2313432

SPIE.

Event: SPIE Astronomical Telescopes + Instrumentation, 2018, Austin, Texas, United States

Concept design of the LiteBIRD satellite for CMB B-mode polarization

Y. Sekimoto^{14,37}, P. Ade², K. Arnold⁴⁹, J. Aumont¹², J. Austermann²⁹, C. Baccigalupi¹¹,
A. Banday¹², R. Banerji⁵⁶, S. Basak^{7,11}, S. Beckman⁴⁹, M. Bersanelli⁴⁴, J. Borrill²⁰,
F. Boulanger⁴, M.L. Brown⁵³, M. Bucher¹, E. Calabrese², F.J. Casas¹⁰, A. Challinor^{50,60,64},
Y. Chinone^{16,47}, F. Columbro⁴⁶, A. Cukierman^{47,36}, D. Curtis⁴⁷, P. de Bernardis⁴⁶, M. de
Petris⁴⁶, M. Dobbs²³, T. Dotani^{14,37}, L. Duband³, JM. Duval³, A. Ducout¹⁶, K. Ebisawa¹⁴,
T. Elleflot⁴⁹, H. Eriksen⁵⁶, J. Errard¹, R. Flauger⁴⁹, C. Franceschet⁵⁴, U. Fuskeland⁵⁶,
K. Ganga¹, J.R. Gao³⁵, T. Ghigna^{16,57}, J. Grain⁹, A. Gruppuso⁶, N. Halverson⁵¹, P. Hargrave²,
T. Hasebe¹⁴, M. Hasegawa^{5,37}, M. Hattori⁴², M. Hazumi^{5,14,16,37}, S. Henrot-Versille¹⁹,
C. Hill^{21,47}, Y. Hirota³⁸, E. Hivon⁶¹, D.T. Hoang^{1,63}, J. Hubmayr²⁹, K. Ichiki²⁴, H. Imada¹⁹,
H. Ishino³⁰, G. Jaehnig⁵¹, H. Kanai⁵⁹, S. Kashima²⁵, Y. Kataoka³⁰, N. Katayama¹⁶,
T. Kawasaki¹⁷, R. Kesitalo^{20,48}, A. Kibayashi³⁰, T. Kikuchi¹⁴, K. Kimura³¹, T. Kisner^{20,48},
Y. Kobayashi³⁹, N. Kogiso³¹, K. Kohri⁵, E. Komatsu²², K. Komatsu³⁰, K. Konishi³⁹,
N. Krachmalnicoff¹¹, C.L. Kuo^{34,36}, N. Kurinsky^{34,36}, A. Kushino¹⁸, L. Lamagna⁴⁶,
A.T. Lee^{21,47}, E. Linder^{21,48}, B. Maffei⁹, M. Maki⁵, A. Mangilli¹², E. Martinez-Gonzalez¹⁰,
S. Masi⁴⁶, T. Matsumura¹⁶, A. Mennella⁵⁴, Y. Minami⁵, K. Mistuda¹⁴, D. Molinari^{52,6},
L. Montier¹², G. Morgante⁶, B. Mot¹², Y. Murata¹⁴, A. Murphy²⁸, M. Nagai²⁵, R. Nagata⁵,
S. Nakamura⁵⁹, T. Namikawa²⁷, P. Natoli⁵², T. Nishibori¹⁵, H. Nishino⁵, F. Noviello²,
C. O'Sullivan²⁸, H. Ochi⁵⁹, H. Ogawa³¹, H. Ogawa¹⁴, H. Ohsaki³⁸, I. Ohta⁵⁸, N. Okada³¹,
G. Patanchon¹, F. Piacentini⁴⁶, G. Pisano², G. Polenta¹³, D. Poletti¹¹, G. Puglisi³⁶, C. Raun⁴⁷,
S. Realini⁵⁴, M. Remazeilles⁵³, H. Sakurai³⁸, Y. Sakurai¹⁶, G. Savini⁴³, B. Sherwin^{50,64,21},
K. Shinozaki¹⁵, M. Shiraishi²⁶, G. Signorelli⁸, G. Smecher⁴¹, R. Stompor¹, H. Sugai¹⁶,
S. Sugiyama³², A. Suzuki²¹, J. Suzuki⁵, R. Takaku^{14,40}, H. Takakura^{14,39}, S. Takakura¹⁶,
E. Taylor⁴⁸, Y. Terao³⁸, K.L. Thompson^{34,36}, B. Thorne⁵⁷, M. Tomasi⁴⁴, H. Tomida¹⁴,
N. Trappe²⁸, M. Tristram¹⁹, M. Tsuji²⁶, M. Tsujimoto¹⁴, S. Uozumi³⁰, S. Utsunomiya¹⁶,
N. Vittorio⁴⁵, N. Watanabe¹⁷, I. Wehus⁵⁶, B. Westbrook⁴⁷, B. Winter⁶², R. Yamamoto¹⁴,
N.Y. Yamasaki¹⁴, M. Yanagisawa³⁰, T. Yoshida¹⁴, J. Yumoto³⁸, M. Zannoni⁵⁵, A. Zonca³³

¹AstroParticle and Cosmology (APC) - University Paris Diderot, CNRS/IN2P3, CEA/Irfu,
Obs de Paris, Sorbonne Paris Cité, France

²Cardiff University, School of Physics and Astronomy, Cardiff CF10 3XQ, UK

³Univ. Grenoble Alpes, CEA, INAC-SBT, 38000 Grenoble, France

⁴Ecole Normale Supérieure

⁵High Energy Accelerator Research Organization (KEK), Tsukuba, Ibaraki 305-0801, Japan

⁶INAF - OAS Bologna, via Piero Gobetti, 93/3, 40129 Bologna (Italy)

⁷School of Physics, Indian Institute of Science Education and Research Thiruvananthapuram,
Maruthamala PO, Vithura, Thiruvananthapuram 695551, Kerala, India

⁸INFN Sezione di Pisa, Largo Bruno Pontecorvo 3, 56127 Pisa (Italy)

⁹Institut d'Astrophysique Spatiale (IAS), CNRS, UMR 8617, Université Paris-Sud 11,
Bâtiment 121, 91405 Orsay, France

¹⁰Instituto de Física de Cantabria (IFCA, CSIC-UC), Avenida los Castros SN, 39005,
Santander, Spain

¹¹International School for Advanced Studies (SISSA), Via Bonomea 265, 34136, Trieste, Italy

- ¹²IRAP, Université de Toulouse, CNRS, CNES, UPS, (Toulouse), France
- ¹³Space Science Data Center, Italian Space Agency, via del Politecnico, 00133, Roma, Italy
- ¹⁴Japan Aerospace Exploration Agency (JAXA), Institute of Space and Astronautical Science (ISAS), Sagamihara, Kanagawa 252-5210, Japan
- ¹⁵Japan Aerospace Exploration Agency (JAXA), Research and Development Directorate, Tsukuba, Ibaraki 305-8505, Japan
- ¹⁶Kavli Institute for the Physics and Mathematics of the Universe (Kavli IPMU, WPI), UTIAS, The University of Tokyo, Kashiwa, Chiba 277-8583, Japan
- ¹⁷Kitasato University, Sagamihara, Kanagawa 252-0373, Japan
- ¹⁸Kurume University, Kurume, Fukuoka 830-0011, Japan
- ¹⁹Laboratoire de l'Accélérateur Linéaire (LAL), Univ. Paris-Sud, CNRS/IN2P3, Université Paris-Saclay, Orsay, France
- ²⁰Lawrence Berkeley National Laboratory (LBNL), Computational Cosmology Center, Berkeley, CA 94720, USA
- ²¹Lawrence Berkeley National Laboratory (LBNL), Physics Division, Berkeley, CA 94720, USA
- ²²Max-Planck-Institut for Astrophysics, D-85741 Garching, Germany
- ²³McGill University, Physics Department, Montreal, QC H3A 0G4, Canada
- ²⁴Nagoya University, Kobayashi-Maskawa Institute for the Origin of Particle and the Universe, Aichi 464-8602, Japan
- ²⁵National Astronomical Observatory of Japan, Mitaka, Tokyo 181-8588, Japan
- ²⁶National Institute of Technology, Kagawa College
- ²⁷National Taiwan University
- ²⁸National University of Ireland Maynooth
- ²⁹National Institute of Standards and Technology (NIST), Boulder, Colorado 80305, USA
- ³⁰Okayama University, Department of Physics, Okayama, Okayama 700-8530, Japan
- ³¹Osaka Prefecture University, Sakai, Osaka 599-8531, Japan
- ³²Saitama University, Saitama 338-8570, Japan
- ³³San Diego Supercomputer Center, University of California, San Diego, La Jolla, California, USA
- ³⁴SLAC National Accelerator Laboratory, Kavli Institute for Particle Astrophysics and Cosmology (KIPAC), Menlo Park, CA 94025, USA
- ³⁵SRON Netherlands Institute for Space Research
- ³⁶Stanford University, Department of Physics, CA 94305-4060, USA
- ³⁷The Graduate University for Advanced Studies (SOKENDAI), Miura District, Kanagawa 240-0115, Hayama, Japan
- ³⁸The University of Tokyo, Tokyo 113-0033, Japan
- ³⁹The University of Tokyo, Department of Astronomy, Tokyo 113-0033, Japan
- ⁴⁰The University of Tokyo, Department of Physics, Tokyo 113-0033, Japan
- ⁴¹Three-Speed Logic, Inc.
- ⁴²Tohoku University, Graduate School of Science, , Astronomical Institute, Sendai, 980-8578, Japan
- ⁴³Optical Science Laboratory, Physics and Astronomy Dept., University College London (UCL)
- ⁴⁴Dipartimento di Fisica, Università degli Studi di Milano, INAF-IASF Milano, and Sezione INFN Milano
- ⁴⁵Dipartimento di Fisica, Università di Roma "Tor Vergata", and Sezione INFN Roma2

- ⁴⁶Dipartimento di Fisica, Università La Sapienza, P. le A. Moro 2, Roma, Italy and INFN Roma
- ⁴⁷University of California, Berkeley, Department of Physics, Berkeley, CA 94720, USA
- ⁴⁸University of California, Berkeley, Space Science Laboratory, Berkeley, CA 94720, USA
- ⁴⁹University of California, San Diego, Department of Physics, San Diego, CA 92093-0424, USA
- ⁵⁰DAMTP, Centre for Mathematical Sciences, Wilberforce Road, Cambridge CB3 0WA, U.K.
- ⁵¹University of Colorado Boulder, Department of Physics and Center for Astrophysics and Space Astronomy, CO 80309, USA
- ⁵²Dipartimento di Fisica e Scienze della Terra, Università di Ferrara and Sezione INFN di Ferrara, Via Saragat 1, 44122 Ferrara, Italy
- ⁵³University of Manchester, Manchester M13 9PL, United Kingdom
- ⁵⁴University of Milano, and Sezione INFN Milano
- ⁵⁵University of Milano Bicocca, Physics Department, p.zza della Scienza, 3, 20126 Milan Italy
- ⁵⁶University of Oslo, Institute of Theoretical Astrophysics, University of Oslo, NO-0315 Oslo, Norway
- ⁵⁷University of Oxford
- ⁵⁸ Konan University, Faculty of Science and Engineering, Hyogo 658-8501, Japan
- ⁵⁹Yokohama National University, Yokohama, Kanagawa 240-8501, Japan
- ⁶⁰Institute of Astronomy, Madingley Road, Cambridge CB3 0HA, U.K.
- ⁶¹ Institut d ' Astrophysique de Paris, CNRS/Sorbonne Université, Paris France
- ⁶² Mullard Space Science Laboratory, University College London, London
- ⁶³ Department of Space and Aeronautics, University of Science and Technology of Hanoi (USTH), Vietnam Academy of Science and Technology (VAST), Hanoi, Vietnam
- ⁶⁴Kavli Institute for Cosmology Cambridge, Madingley Road, Cambridge CB3 0HA, U.K.

ABSTRACT

LiteBIRD is a candidate for JAXA's strategic large mission to observe the cosmic microwave background (CMB) polarization over the full sky at large angular scales. It is planned to be launched in the 2020s with an H3 launch vehicle for three years of observations at a Sun-Earth Lagrangian point (L2). The concept design has been studied by researchers from Japan, U.S., Canada and Europe during the ISAS Phase-A1. Large scale measurements of the CMB B-mode polarization are known as the best probe to detect primordial gravitational waves. The goal of LiteBIRD is to measure the tensor-to-scalar ratio (r) with precision of $\delta r < 0.001$. A 3-year full sky survey will be carried out with a low frequency (34 - 161 GHz) telescope (LFT) and a high frequency (89 - 448 GHz) telescope (HFT), which achieve a sensitivity of $2.5 \mu\text{K-arcmin}$ with an angular resolution of ~ 30 arcminutes around 100 GHz. The concept design of LiteBIRD system, payload module (PLM), cryo-structure, LFT and verification plan is described in this paper.

Keywords: Cosmic microwave background, space program, millimeter-wave polarization, cryogenic telescope

1. INTRODUCTION

LiteBIRD, Lite (Light) satellite for the studies of B-mode polarization and Inflation from cosmic background Radiation Detection, observes the cosmic microwave background (CMB) polarization over the full sky at large angular scales.¹⁻⁵ Cosmological inflation predicts primordial gravitational waves, which imprinted large-scale curl (B-mode) patterns in the CMB polarization map.⁶⁻⁹ Measurements of the CMB B-mode signals are known as the best probe to detect the primordial gravitational waves and to measure the inflation energy. The scientific objective of LiteBIRD is to test major inflationary models.¹⁰ The power of the B-modes is proportional to the

Send correspondence to Yutaro Sekimoto, E-mail: sekimoto.yutaro@jaxa.jp

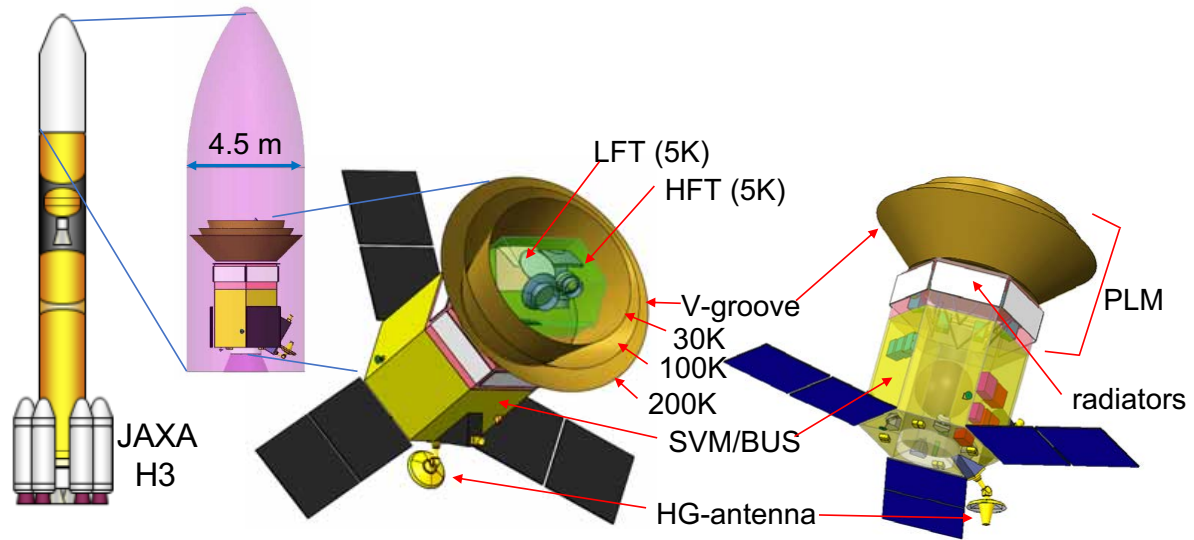


Figure 1. The LiteBIRD spacecraft

tensor-to-scalar ratio, r . The current upper limit on r is $r < 0.07$.¹¹ The mission goal of LiteBIRD is to measure r with a precision of $\delta r < 0.001$, which provides a crucial test of the cosmic inflation. The required angular coverage is $2 < l < 200$, where l (ell) is the multipole moment.

LiteBIRD is a candidate for JAXA's strategic large mission. LiteBIRD has been endorsed as one of the prioritized projects in the master plan 2017 by the Science Council of Japan. A down-selection by ISAS is planned around late 2018 ~ early 2019. It is scheduled to be launched around 2027 with an H3 vehicle for three years of observations at a Lagrangian point (L2) of the Earth-Sun system. The concept design has been studied by researchers from Japan, U.S., Canada, and Europe since September 2016. This proceedings presents a part of the concept design. Details of the cryo-system,¹² electric system,¹³ focal plane,¹⁴ LFT optics,¹⁵ and HWP¹⁶ of LiteBIRD are separately reported.

2. SYSTEM DESIGN

Requirements flow down from science goal of $\delta r = 0.001$. This requirement is equally divided into three; statistical uncertainty of less than $\delta r = 5.7 \times 10^{-4}$, systematic uncertainty of less than $\delta r = 5.7 \times 10^{-4}$, and a margin of $\delta r = 5.7 \times 10^{-4}$. The statistical uncertainty includes uncertainties of lensing B-mode and foregrounds subtraction.

One advantage of a space program for CMB B-mode polarization detection is foreground subtraction, which is studied with broadband and large angles. Several approaches have been investigated for LiteBIRD.¹⁷⁻²¹ These studies found that it can be marginal to achieve $\delta r = 5.7 \times 10^{-4}$ with the 2016 baseline sensitivity presented at the last SPIE 2016 at Edinburgh.⁴ So we have designed an enhanced HFT; both HFT and LFT have equal bandwidth of 1:5.

There are many sources of systematic errors. Each item of the errors contributes to be less than 1 % of $\delta r = 5.7 \times 10^{-4}$. The HWP can reduce differential systematic errors, including with beam patterns, gain, and bandpass.²² On the other hand, the HWP itself can produce the systematic errors²³ and the study is in progress.

The LiteBIRD spacecraft is shown in Figure 1. The block diagram depicting the preliminary task sharing of LiteBIRD is shown in Figure 2. The spacecraft is composed of payload module (PLM) and service module (SVM). The PLM consists of high frequency and low frequency telescopes, with their respective focal planes, and cryo-structure and room-temperature part of PLM. The cryo-structure is made of active cooling chain including sub-K cooler and passive cooling (V-groove), and mechanical structures. The basic parameters of LiteBIRD are tabulated in Table 1.

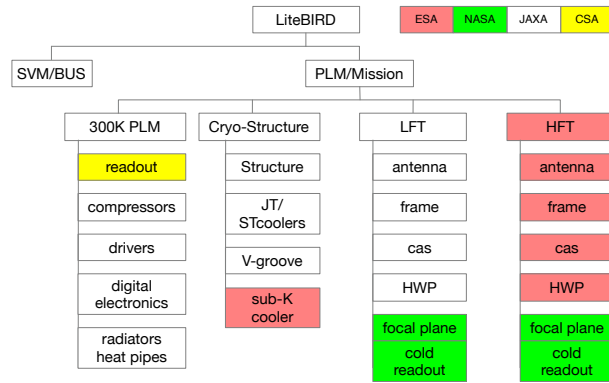


Figure 2. Preliminary work sharing of LiteBIRD. Red, green, and yellow indicate European, US and Canada contributions, respectively. cas: cold aperture stop.

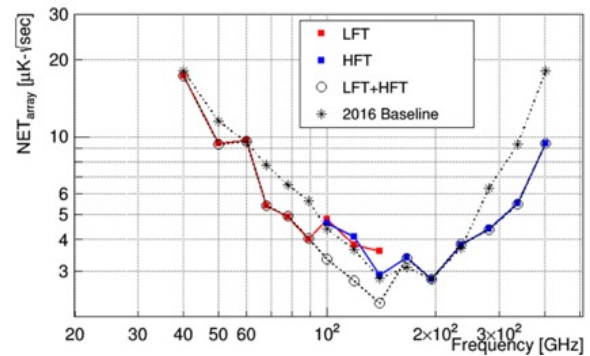


Figure 3. Sensitivity of LiteBIRD. The 2016 Baseline sensitivity was reported in Ishino et al.⁴

The design and operation of the LiteBIRD satellite are driven by requirements, which derive from the top requirement of $\delta r = 0.001$. A 3-year full sky survey will be carried out with LFT (34 - 161 GHz) and HFT (89 - 448 GHz) to achieve the unprecedented sensitivity (Figure 3 and Table 2). The mission instruments are cooled down below 5 K with mechanical cryocoolers and a passive cooling system.

Due to the limited bandwidth of a half-wave plate for polarization modulation, LiteBIRD has two telescopes: a reflective low-frequency telescope with an aperture of 40 cm and a high-frequency telescope with an aperture of 30 cm. The angular resolution of each band is tabulated in Table 2. Both telescopes have polarization-sensitive multi-choric TES array detector operated at 100 mK.¹⁴

The LiteBIRD mission plan envisions three years of observations at the Sun-Earth Lagrangian 2 point. It is a spinning satellite with a precession angle (α) of 45 degrees and spin angle (β) of 50 degrees with spin rate of 0.1 rpm and precession period of 93 minutes, which are optimized from crossing angles and revisits of previously scanned regions.

The BUS or service module (SVM) of LiteBIRD is shown in Figure 1. The SVM supports scan, pointing, power supply and communication as specified in Table 1. The mass and electrical power of LiteBIRD are 2.6 tons and 3.0 kW, respectively. The breakdown is tabulated in Table 3. The mass and electrical power of SVM include a 10 % margin. The mass and electrical power of PLM include a 20 % margin. The electronics system design of LiteBIRD has been reported by Tsujimoto et al.¹³

The power consumption of cooler compressors and drivers is about 1.5 kW, which is transferred to radiators with heat pipes. The area of the radiators is required to be around 10 m², so most outer panels of 300K PLM and some part of upper surface of SVM are used as radiators.

The data transfer and telecommunication are planned with a new JAXA 54 m ground station, GREAT (Ground station for deep space Exploration And Tele-communication), which is under construction near the USUDA 64 m station, Nagano prefecture, Japan.

3. PAYLOAD MODULE

Requirements for payload module have been derived from the top-level requirement of achieving a tensor-to-scalar ratio error of $\delta r = 0.001$. LiteBIRD observes millimeter waves from 34 GHz to 448 GHz with two telescopes, LFT and HFT. A HWP for polarization modulation has a limited bandwidth, and so LiteBIRD has two telescopes to cover the frequency bands as defined in Table 4. This focal plane design is based on multi-choric TES at 100 mK operation.¹⁴

The frequency coverages of LFT and HFT have been modified after the last SPIE conference^{4,24}. Both telescopes have equal 1:5 band coverage: LFT observes Synchrotron and CMB bands, and HFT covers both CMB and dust bands. The CMB bands of 89 - 161 GHz are overlapped to reduce systematics associated with

Table 1. LiteBIRD basic parameters

| | Low Frequency Telescope (LFT) | High Frequency Telescope (HFT) |
|---------------------|--|--------------------------------|
| Frequency | 34 ~ 161 GHz | 89 ~ 448 GHz |
| field of view | > 20 deg × 10 deg | > 20 deg × 10 deg |
| aperture diameter | 400 mm | 300 mm |
| angular resolution | 20 ~ 70 arcmin | 10 ~ 40 arcmin |
| rotational HWP | 88 rpm | 170 rpm |
| number of detectors | ~1000 | ~2100 |
| data sampling rate | 22 Hz | 46 Hz |
| Uncertainty of r | $\delta r < 1 \times 10^{-3}$ | |
| Observation period | 3 years | |
| Scan | L2 Lissajous, precession angle 45 deg, spin angle 50 deg (0.1 rpm) | |
| Sensitivity | $< 3 \mu\text{K} \cdot \text{arcmin}$ | |
| pointing knowledge | $< 3 \text{ arcmin}$ | |
| focal plane array | bath temperature 100 mK $\text{NET}_{\text{array}}^P = 1.7 \mu\text{K} \cdot \sqrt{s}$ detector $f_{\text{knee}} < 20 \text{ mHz}$ | |
| data transfer | 7 GByte/day | |
| mass | 2.6 ton | |
| electrical power | 3.0 kW | |

Table 2. Sensitivity and beam size of LiteBIRD

| Band GHz | NET array $\mu\text{K} \cdot \text{s}^{1/2}$ | LFT | | HFT | | polarization sensitivity $\mu\text{K} \cdot \text{arcmin}$ |
|-------------|---|---------------------|--|---------------------|--|--|
| | | beam size arcmin | NET _{array} $\mu\text{K} \cdot \text{s}^{1/2}$ | beam size arcmin | NET _{array} $\mu\text{K} \cdot \text{s}^{1/2}$ | |
| 40 | 13.4 | 69.2 | 13.4 | | | 27.9 |
| 50 | 9.4 | 56.9 | 9.4 | | | 19.6 |
| 60 | 7.5 | 49.0 | 7.5 | | | 15.6 |
| 68 | 5.9 | 40.8 | 5.9 | | | 12.3 |
| 78 | 4.8 | 36.1 | 4.8 | | | 10.0 |
| 89 | 4.5 | 32.3 | 4.5 | | | 9.4 |
| 100 | 3.7 | 27.7 | 5.9 | 37.0 | 4.6 | 7.6 |
| 119 | 3.0 | 23.7 | 4.6 | 31.6 | 4.1 | 6.4 |
| 140 | 2.4 | 20.7 | 4.4 | 27.6 | 2.9 | 5.1 |
| 166 | 3.4 | | | 24.2 | 3.4 | 7.0 |
| 195 | 2.8 | | | 21.7 | 2.8 | 5.8 |
| 235 | 3.8 | | | 19.6 | 3.8 | 8.0 |
| 280 | 4.4 | | | 13.2 | 4.4 | 9.1 |
| 337 | 5.5 | | | 11.2 | 5.5 | 11.4 |
| 402 | 9.4 | | | 9.7 | 9.4 | 19.6 |

Table 3. Mass and power estimates of LiteBIRD

| | mass [kg] | electrical power [W] |
|-------------------------------------|--------------|-------------------------|
| 5K PLM | 260 | |
| LFT | 148 | |
| HFT | 91 | |
| sub-K cooler | 7 | |
| margin | 14 | |
| Structure | 188.4 | |
| truss | 71.4 | |
| V-groove | 107 | |
| harness | 4 | |
| He pipes | 6 | |
| Coolers and compressors | 297 | |
| ST coolers | 86 | 450 |
| JT cooler compressors | 86 | 165 |
| base, radiators | 125 | |
| Cooler drivers | 149 | |
| ST drivers | 110 | 651 |
| JT drivers | | 280 |
| sub-K driver | 39 | 26 |
| Electronics | 44 | |
| HWP controller | 5.2 | 52 |
| house keeping | 5.2 | 26 |
| data compression electronics | 28 | 26 |
| warm electronics unit | | 172 |
| squid controller | | |
| power distribution unit | 6 | 20 |
| M-SWR (14port) | | 5 |
| Radiator/heaters | 108 | |
| MLI, heaters, sensors | 15.4 | |
| radiator/heat pipes | 93 | |
| 300K PLM sum | 787 | 1873 |
| 300K PLM sum + 20 % margin + 5K PLM | 1204 | 2247 |
| SVM (including 10 % margin) | 1357 | 715 |
| Total | 2561 | 2962 |

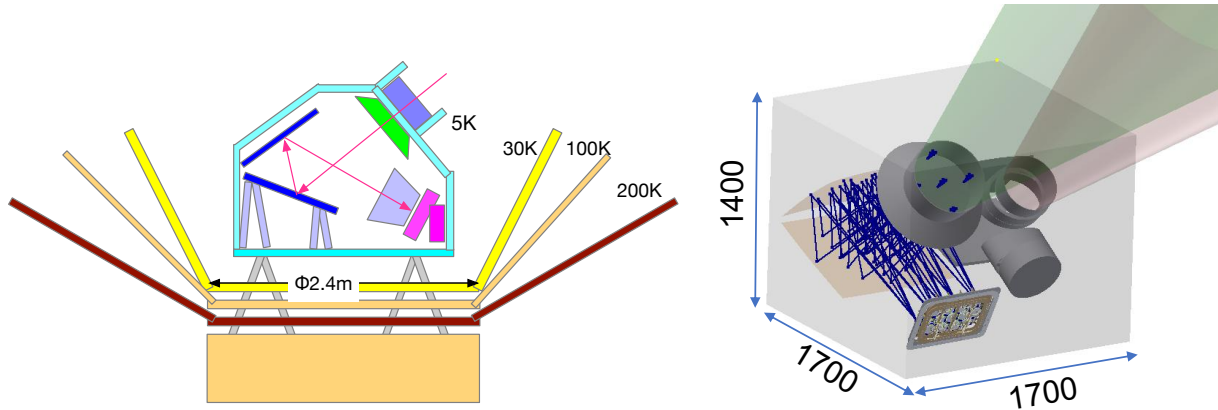


Figure 4. Left: a cartoon of the payload module (PLM) including 300 K part. Right : LFT and HFT. This LFT drawing shows cold aperture stop (CAS), two mirrors and the focal plane array. HFT is the smaller one. The envelope of LFT and HFT is less than 1.7 m × 1.7 m × 1.4 m height.

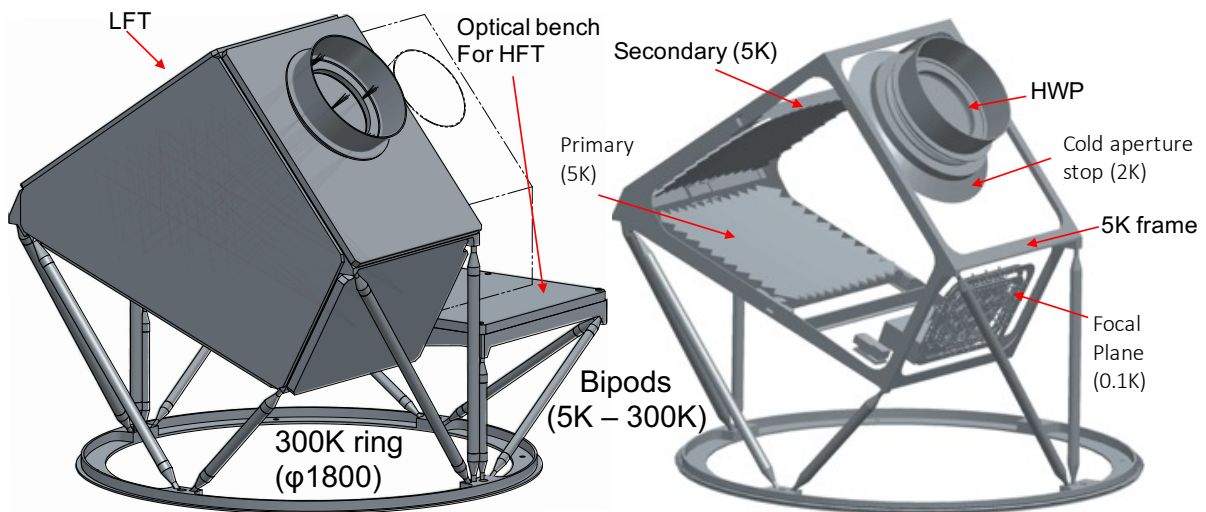


Figure 5. LFT and its support structure. There is a 5K optical bench for HFT in the back side. The outmost of both telescopes is less than 1.7 m × 1.7 m × 1.4 m height. LFT and HFT have apertures of 400 and 300 millimeter, respectively. The right-side panel shows the low frequency antenna design, which is supported from the 300K ring ($\phi = 1800$ mm) by bipods.

the telescope and as a redundancy. A design of LFT and PLM is shown in Figure 5. Both telescopes are cooled down to 5K. The major requirements on the PLM of LiteBIRD are tabulated in Table 5.

LFT has an aperture of 40 cm, and HFT has an aperture of 30 cm. The envelope of LFT and HFT is less than 1.7 m × 1.7 m × 1.4 m height. This size should be kept as small as possible, because the radiative cooling power of a non-expandable V-groove is dependent on the opening angle. The weights of LFT and HFT are expected to be 148 kg and 91 kg, respectively. This is also kept as light as possible, because the thermal conductivity of the support truss depends on the mass.

HFT has been designed by the European consortium and the European Space Agency (ESA). Current baseline design of HFT is a reflective antenna with a reflective HWP. The broadband capability of the reflective HWP has been demonstrated.²⁵ An optical design of the HFT has been presented by Hasebe et al.²⁶

4. LOW FREQUENCY TELESCOPE (LFT)

Challenges of LiteBIRD are wide field-of-view (FoV) and broadband capabilities of millimeter-wave polarization measurements, which are derived from the sensitivity requirements. The wide FoV corresponds to a large focal plane area; a detector pixel has different spill-over or edge-taper depending on the pixel position on the focal plane. Possible paths of stray light increase with a wider FoV. The broad-band (1:5) capability requires different frequency modules. Current planar band-pass filter technology has limited bandwidth, so for example, one frequency module receives 40 GHz, but the higher frequency modules reflect 40 GHz (see Table 4). There are many band edges, where the feed pattern may distort. The telescope has many reflection paths among FP, CAS, HWP, among quasi-optical LP Filters. The absorbers covering the optics and the focal plane are not ideal and they have frequency dependence as well as angle dependence of reflectance. These challenges shall be overcome by design and demonstrations.

After various trade-off studies of various optical configurations including a front-fed Dragone,²⁷ we concluded that the crossed Dragone antenna is the best option for LiteBIRD. Wide FoV design of a crossed Dragone antenna has been studied by Kashima et al. 2018.²⁸ A ray diagram of LFT is shown in Figure 6, which has an FoV of 20 degrees \times 10 degrees. The F#3.0 and the crossing angle of optical axes of 90 degrees are chosen after an extensive study of stray light. We found that "clipped" side lobe²⁹ or triple reflection¹⁵ of the crossed Dragone optics can be avoided with this configuration. Primary and secondary mirrors have rectangular shape (\sim 900 mm \times 800 mm) with serrations to reduce diffraction pattern from the edges of mirrors. An optimization for the serration pattern has been reported.³⁰ The far sidelobe knowledge of -60 dB (see Table 5) is one of challenging requirements. In flight, the calibration accuracy of LiteBIRD is not as good as that of the Planck satellite. The far sidelobe is designed as low as possible in order to predict it from room temperature measurements of the far sidelobes, cryogenic measurements of near sidelobes, and in-flight calibration of near sidelobes.

Physical optics simulation of LFT with GRASP10³¹ is reported by Imada et al.,¹⁵ the simulated telescope elements including LFT reflectors and cold aperture stop. At this stage, the HWP, which may generate additional side-lobes, is not taken into account for the physical optics simulation. LiteBIRD is more challenging for modeling the optics than Planck.³² It is necessary to take into account following items: (1) absorbers on enclosures, aperture stops, hoods, baffles; (2) broadband feeds with lower return loss and larger side lobes; (3) HWP effects including the rotation mechanism on the beam.

There is a trade-off of mechanical structure in LFT between a frame type and an optical bench type. A frame-type design of LFT is shown in Figure 5. The frame and LF mirrors are made of aluminum in order to shrink similarly to 5 K. The mass of LFT including the focal plane is estimated to \sim 150 kg. The frame is supported by trusses made of CFRP via a kinematic mount to release thermal stress.

In the optical bench configuration as shown in Figure 4, the LF-antenna, 5K enclosure and the focal plane are independently supported on the optical bench. The 5K enclosure supports the HWP and cold aperture stop. The 5K frame plays the roles of an optical bench, 5K enclosure, and support for LF mirrors, and thus the mass of LFT can be reduced. There is a concern on possible distortion of the 5K frame by thermoelastic effect of absorbers or the rotating HWP. The absorber, made of plastic/carbon is adhered to a panel with epoxy, then the panel is fixed to the 5K frame. The cryogenic contraction of the absorber and the epoxy is a potential source of thermal deformation of the antenna. If there is non-uniformity of mass distribution of the HWP at 88 r.p.m., the HWP may be a possible source of distortion. The optical bench can mitigate such distortions. From the view point of verification and tests, the frame architecture can be used as an LF antenna structure. The 5K frame has a position reference for the focal plane and the HWP. The current baseline of HWP is a transmissive one, then extremely precise alignment is not required. In the case of reflective HWP, very precise alignment between the mirrors and HWP is required.

The 5 K frame is directly connected by the trusses, which have a temperature gradient from 300K to 5K and a finite thermal expansion coefficient. Because the trusses for the 5K frame architecture have different lengths, this can be a possible source for cryogenic deformation of the crossed Dragone antenna, but it can be mitigated by measuring the thermal expansion coefficient.

A transmissive sapphire HWP has been developed for LiteBIRD.^{16,33} The HWP is placed as the first optical element of the telescope, which is in front of the cold aperture stop or entrance pupil. The HWP is inclined at 5

Table 4. Frequency bands and detector configuration. The CO lines are avoided with planar notch filters. This table shows only optical TESs. There are additional dark TESs for the monitor purpose.

| | Type | Center [GHz] | BW | Low [GHz] | High [GHz] | Num. of wafers | TES channels | | |
|------------------|------------------|--------------|------|-----------|------------|----------------|--------------|-------|------|
| | | | | | | | Opt/wf | Total | |
| LFT 34 - 161 GHz | 1 | 40 | 0.30 | 34 | 46 | 3 | 14 | 42 | |
| | | 60 | 0.23 | 53 | 67 | 3 | 14 | 42 | |
| | | 78 | 0.23 | 69 | 87 | 3 | 14 | 42 | |
| | 2 | 50 | 0.30 | 43 | 58 | 4 | 14 | 56 | |
| | | 68 | 0.23 | 60 | 76 | 4 | 14 | 56 | |
| | | 89 | 0.23 | 79 | 99 | 4 | 14 | 56 | |
| | 3 | 68 | 0.23 | 60 | 76 | 3 | 38 | 114 | |
| | | 89 | 0.23 | 79 | 99 | 3 | 38 | 114 | |
| | 4 | 119 | 0.30 | 101 | 137 | 3 | 38 | 114 | |
| | | 78 | 0.23 | 69 | 87 | 3 | 38 | 114 | |
| | | 100 | 0.23 | 89 | 112 | 3 | 38 | 114 | |
| | HFT 89 - 448 GHz | 5 | 140 | 0.30 | 119 | 161 | 3 | 74 | 222 |
| 195 | | | 0.30 | 166 | 224 | 3 | 74 | 222 | |
| 235 | | | 0.30 | 200 | 270 | 2 | 74 | 148 | |
| 6 | | 119 | 0.30 | 101 | 137 | 2 | 74 | 148 | |
| | | 166 | 0.30 | 141 | 191 | 2 | 74 | 148 | |
| | | 235 | 0.30 | 200 | 270 | 2 | 74 | 148 | |
| 7 | | 235 | 0.30 | 200 | 270 | 1 | | | |
| | | 337 | 0.30 | 286 | 388 | 1 | 338 | 338 | |
| 8 | | 280 | 0.30 | 238 | 322 | 1 | 338 | 338 | |
| | | 402 | 0.23 | 356 | 448 | 1 | 338 | 338 | |
| Total | | | | | | | | | 3102 |
| LFT | | | | | | | | | 978 |
| HFT | | | | | | | | 2124 | |

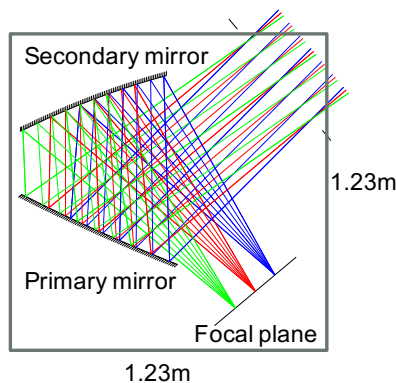


Figure 6. Ray trace of LFT crossed Dragone optics with an aperture diameter of 400 mm and FoV of 20 degrees \times 10 degrees. The optical configuration is F#3.0 and the crossing angle of the optical axes of 90 degree.

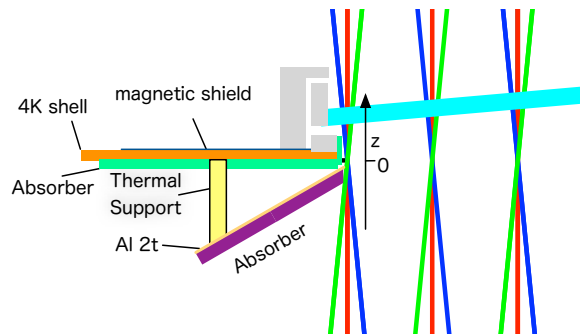


Figure 7. A design of cold aperture stop at 2 K. The HWP is inclined at 5 degrees.

Table 5. Major requirements of PLM and verification methods. CT represents cryogenic test, A analysis, T room temperature test. DM: demonstration model, STM: structure thermal model, EM: engineering model, FM: flight model.

| Requirements | | Method | Model | method |
|--------------------------------------|----------------------|--------|-------------|----------------------------|
| Instrument Sensitivity | Table 2 | CT | DM, EM, FM | hot-cold |
| Spectral optical response | 0.10% | CT | DM, FM | CW/FTS |
| Band definitions | Table 4 | CT | DM, FM | CW/FTS |
| Data loss due to Cosmic rays | 5% | A | DM, EM, FM | hot-cold |
| Operating life of instruments | 3 years | A, CT | DM, EM | |
| Post demodulation 1/f noise | $f_{knee} < 0.2$ mHz | CT | DM, EM, FM | rotating wire grid |
| Modulation synchronous instr. pol. | < 0.03 % | CT | DM, FM | rotating wire grid |
| Far sidelobe knowledge | -60dB(diffuse) | T, A | DM, FM | compact range |
| Near sidelobe knowledge | TBD | CT | DM, FM | phase retrieval near field |
| Beam flattening | < 15 % | CT | DM, FM | phase retrieval near field |
| Response non-linearity | TBD | CT | DM, EM, FM | hot-cold |
| Gain variation in time (single det.) | < 10 % (600sec) | CT | DM, EM, FM | hot-cold |
| Linear pol. responsivity | TBD | CT | DM, FM | rotating wire grid |
| Pointing offset knowledge | < 3 arcmin | CT, A | DM, FM | phase retrieval near field |
| Abs. pol. angle knowledge | < 3 arcmin | CT | DM, FM | rotating wire grid |
| Cooling capability | | CT | STM, EM, FM | |
| Mechanical properties | | T, A | STM, EM, FM | standard tests |

degrees to mitigate multiple reflections including optical ghost between the HWP and the focal plane. The HWP uses superconducting magnet for levitation. The eddy current and magnetic hysteresis dissipate and increase the temperature of rotating HWP from 5 K to 10 K. The re-cooling of HWP synchronizes to the re-cycling of the sub kelvin cooler.

A design of the cold aperture stop at 2.0 K with inner and outer diameters of 400 mm and 800 mm, respectively, is shown in Figure 7. This works to make good beam shape and to reduce the photon noise for relatively low edge taper of ~ 3 dB configuration. It is thermally isolated from the 5K structure with CFRP pipes. A millimeter absorber, TK-RAM,^{34,35} is attached on Aluminum cone, which is connected to 1.8 K stage with thermal strap. The weight of the cold aperture stop including the absorber is estimated to be 7 kg. The first eigen frequency of the cold aperture stop was analyzed to be 120 Hz. The heat load to the 1.8K stage is around 2.0 mW including heaters to stabilize the temperature to less than 0.2 mK peak-to-peak.

Millimeter absorbers to reduce reflections are attached on the inside surface of the 5K frame, which plays an role of a cavity. Eccosorb AN72 and HR10 are candidates of such absorber, however, they have large TML (total mass loss) and CVCM (collected volatile condensable materials). According to NASA outgass database,³⁶ AN72 washed with ethanol shows reasonable TML and CVCM.

LF focal plane has been described by A. Suzuki et al.¹⁴ The lens and sinuous antenna have broadband capability.³⁷ The focal plane with AlMn TES is cooled to 100 mK. Cosmic ray mitigation has been investigated.³⁸ A quasi-optical metal-mesh low-pass filter³⁹ is put in front of hexagonal modules to reduce thermal loads from the 5 K cavity. The focal plane is covered with a hood to reduce stray light. Magnetic shield to reduce magnetic variation from HWP covers the focal plane except for the optical input.

5. CRYO-STRUCTURE

Thermal design of LiteBIRD is based on studies for SPICA.^{40,41} Cooler configuration composed of active mechanical coolers and passive radiative cooler is shown in Figure 8.

Radiative cooling with V-groove⁴² is efficient especially for Sun-Earth Lagrangian 2 point, as Planck satellite demonstrated efficient passive cooling capability with V-groove.⁴³ The V-groove consists of several cones, whose facing surfaces are not parallel but open for sky. Infrared photons between them are radiated to cold space in a

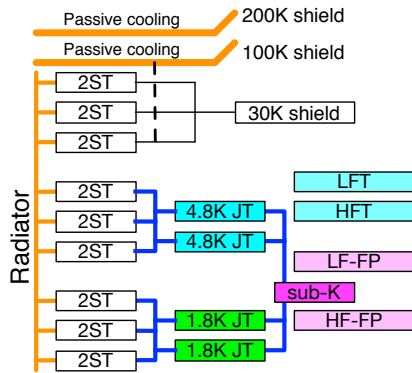


Figure 8. Cooler configuration of LiteBIRD. The V-groove consists of 200K, 100K, and 30K shields. Two coolers of 4.8K JT and 1.8K JT are redundant. 2ST represents 2 stage stirling cooler.

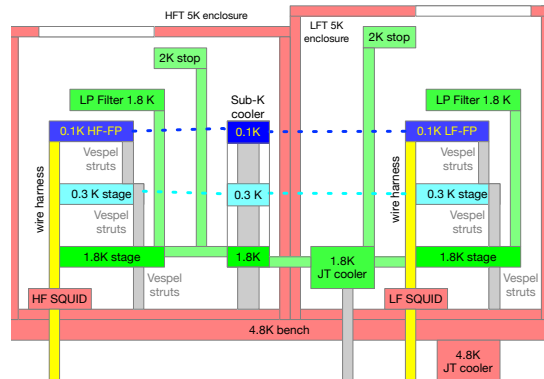


Figure 9. A schematic drawing of 5K part with coolers. HFT and LFT share a sub-Kelvin cooler, 1.8K JT and 4.8K JT coolers.

few reflections. The V-groove has been designed with for the current scan strategy with a spin angle of 50 degrees. Details of the thermal design are described by Hasebe et al.¹²

Radiative cooling power of the V-groove is roughly proportional to the opening angle/area. The outer circumference of the V-groove is limited by the fairing of the H3 vehicle, 4.5 m, if an expanding/deployment mechanism after the launch is not employed. To keep the current radiative cooling power, the outer circumference of the 5 K enclosure shall be less than a diameter 2.4 m (1.7 m × 1.7 m). We are investigating the possibility to reduce the volume/size of LFT to increase available 4.8K cooling power.

A schematic drawing of the cryogenic design of LFT and HFT is shown in Figure 9. In this figure, one 1.8K JT cooler and one 4.8K JT cooler are drawn as a single functional element, although there are two 1.8K JT coolers and two 4.8K JT coolers as redundancy in Figure 8. The 4.8K-JT and 1.8K-JT coolers have cooling capacities of 40 mW at the 4.8 K stage and 10 mW at the 1.8 K stage, respectively, at the end of life (EOL).⁴¹ The 2ST cooler has cooling capacity of 200 mW at the 20 K stage at the end of life (EOL).⁴¹ Taking into account the 30% margin for these mechanical coolers, available cooling powers at the 4.8 K stage and 1.8 K stage are 30 mW and 7 mW, respectively. The redundancy of the mechanical coolers for SPICA has been studied by Shinozaki et al.⁴¹ The 4.8K JT and 2ST coolers achieved TRL (technical readiness level) 8 and the 1.8K JT cooler did TRL 5.

A candidate for a sub-Kelvin cooler is an ADR/sorption hybrid cooler developed by CEA.⁴⁴ This cooler has been demonstrated with JT/ST coolers by the cooling chain core technology program.⁴⁵ This cooler achieved TRL 6. The hybrid cooler needs recycling phase once per day. The recycling heat load of ~ 10 mW for the 4.8K JT cooler is a bottle neck of the thermal design. To reduce the heat load, there is an option that two hybrid coolers for two telescopes have different recycling phase.

Another candidate for a sub-Kelvin cooler is a closed-cycle dilution refrigerator (CCDR)⁴⁶ developed by Neel institute and IAS. The CCDR is continuously operated, but it requires large cooling power for the 1.8K stage. A program to raise the TRL to 5 is running.

A structure analysis of the whole PLM including V-groove structures predicts the first eigen frequency of 74 Hz and 34 Hz for vertical and horizontal axes, respectively. An estimate of conductive and radiative load to the 5 K cooler is 12 mW. Then, the available cooling power for HWP's of LFT and HFT and sub-Kelvin cooler(s) at 4.8 K is 18 mW. The available cooling power of 7 mW at 1.8K is used for cold aperture stops and focal planes of LFT and HFT.

6. ASSEMBLY, INTEGRATION, AND VERIFICATION (AIV) PLAN

The verification and calibration of a warmly-launched cryogenic telescope on the ground are challenging. After the accident of the Hitomi satellite⁴⁷ in March 2016, JAXA has been carrying out operational reform, which suggests a front heavy assembly, integration, and verification (AIV) plan. It requires that technical challenges of a mission shall be verified before PDR (preliminary design review). Technical challenges of LiteBIRD are (1) sensitive polarization measurement capability and (2) cooling chain down to 0.1K and mechanical support structure.

The Demonstration model (DM) of LFT is fully characterized to verify its millimeter-wave beam and noise performances under the cryogenic environments. The requirements are tested and calibrated as shown in Table 5. A dedicated cryogenic chamber will be built for LFT to measure millimeter polarization performance with phase-retrieval near field beam measurements (eg. Manabe et al.⁴⁸), spectral responses with FTS (Fourier transform spectrometer) or CW (continuous wave) sources, and polarization angles with rotating wire-grid mechanism. An FTS has crude spectral resolution of 1 GHz, in general. LiteBIRD needs fine spectral resolution at synchrotron frequencies or for CO lines. A broadband CW source with an appropriate optical design has fine spectral resolution of 0.01 GHz to measure the spectral response. A candidate of the CW source is a photomixer.^{49,50}

One of the issues of the ground calibration is far sidelobe measurement. It is ideal to measure the far sidelobe pattern in the cryogenic environment with the focal plane, but, it is difficult to prepare the cryogenic test-set within the reasonable cost. In this current plan, the far sidelobe is measured with a representative feed at room temperature. The main lobe and near sidelobes measured at cryogenic temperature are compared with those at room temperature, then the far side lobe at the cryogenic temperature is estimated with auxiliary simulations.

Procedure of LFT assembly, integration and verification (AIV) is as follows: 1) dimensions of the 5K frame are measured with a 3D coordinated measurement machine; 2) primary and secondary mirrors are fixed to the frame. After the reference positions of the mirrors are checked with the 3D coordinated measurement machine, the mirror shape is measured with photogrammetry at both room and cryogenic temperatures. Millimeter beam pattern is measured at room temperature; 3) absorbers and cold aperture stop are fixed to the frame. The millimeter beam is measured at both room and cryogenic temperatures. 4) focal plane is fixed to the frame. The millimeter beam, polarization angle, and spectral response are measured at cryogenic temperature. 5) the HWP is installed into the frame. The millimeter beam, polarization angle, and spectral response are measured at cryogenic temperature. Multiple reflections among HWP, FP, reflector and baffles are extensively studied with LFT DM.

A structure thermal model (STM) of the mission payload is constructed and tested with mechanical coolers down to 0.1K and V-grooves to verify mechanical and thermal interfaces. The STM consists of cryo-structure, dummy LFT and dummy HFT. Standard vibration tests to verify the mechanical interfaces of PLM are planned. Both DM and STM are verified in parallel before PDR in the current schedule.

The STM and DM of LFT will be refurbished and used as an Engineering model (EM). The first integration of PLM including HFT is planned with EM to verify all interfaces. This means that one model of LFT and cryo-system is manufactured and is used for both DM and EM. End-to-end tests of noise and optical efficiency measurements are planned with hot-cold loads in front of the apertures of both telescopes. A topic of EM is EMC/EMI tests with electrical power supplies and HGA (high gain antenna) power amplifiers. SVM (service module/BUS) is manufactured as proto-FM (PFM), so EM doesn't test SVM.

A preliminary integration plan of flight model (FM) is shown in Figure 10. It takes long time to make AIV and calibrations of LFT and HFT, so which are done in parallel.

ACKNOWLEDGMENTS

Authors acknowledge technical contributions and by ESA concurrent design facility (CDF) for LiteBIRD high frequency telescope and sub-Kelvin coolers. This work was supported by ISAS/JAXA phase A1 program and acceleration program of JAXA research and development directorate. This work was partially supported by JSPS/MEXT KAKENHI Grant Numbers JP17H01115, JP17H01125, JP15H05891, JP18K03715, JP17H01125, JP17K14272, JP15H05441.

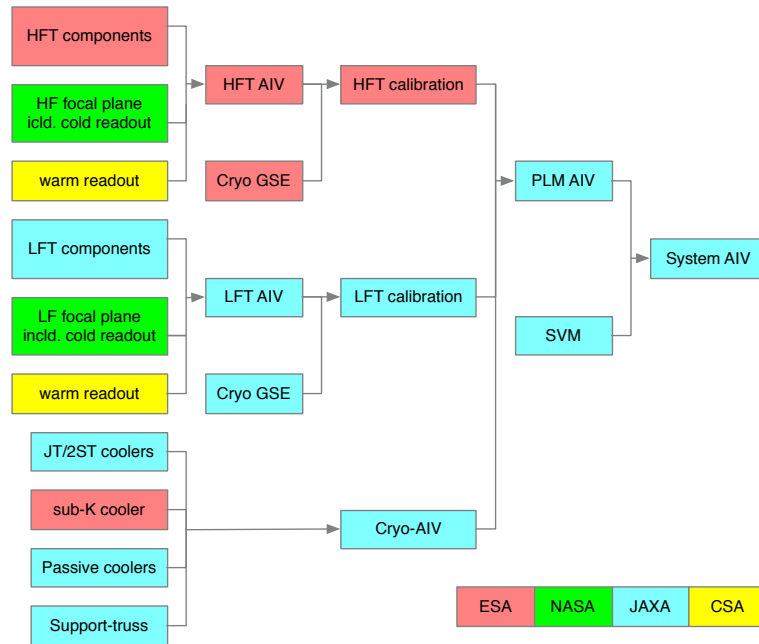


Figure 10. Preliminary integration plan of flight model (FM) of LiteBIRD

REFERENCES

- [1] Hazumi, M., Borrill, J., Chinone, Y., Dobbs, M. A., Fuke, H., Ghribi, A., Hasegawa, M., Hattori, K., Hattori, M., Holzapfel, W. L., Inoue, Y., Ishidoshiro, K., Ishino, H., Karatsu, K., Katayama, N., Kawano, I., Kibayashi, A., Kibe, Y., Kimura, N., Koga, K., Komatsu, E., Lee, A. T., Matsuhara, H., Matsumura, T., Mima, S., Mitsuda, K., Morii, H., Murayama, S., Nagai, M., Nagata, R., Nakamura, S., Natsume, K., Nishino, H., Noda, A., Noguchi, T., Ohta, I., Otani, C., Richards, P. L., Sakai, S., Sato, N., Sato, Y., Sekimoto, Y., Shimizu, A., Shinozaki, K., Sugita, H., Suzuki, A., Suzuki, T., Tajima, O., Takada, S., Takagi, Y., Takei, Y., Tomaru, T., Uzawa, Y., Watanabe, H., Yamasaki, N., Yoshida, M., Yoshida, T., and Yotsumoto, K., "LiteBIRD: a small satellite for the study of B-mode polarization and inflation from cosmic background radiation detection," in [*SPIE Astronomical Telescopes + Instrumentation*], 844219–844219–9 (sep 2012).
- [2] Matsumura, T., Akiba, Y., Borrill, J., Chinone, Y., Dobbs, M., Fuke, H., Hasegawa, M., Hattori, K., Hattori, M., Hazumi, M., Holzapfel, W., Hori, Y., Inatani, J., Inoue, M., Inoue, Y., Ishidoshiro, K., Ishino, H., Ishitsuka, H., Karatsu, K., Kashima, S., Katayama, N., Kawano, I., Kibayashi, A., Kibe, Y., Kimura, K., Kimura, N., Komatsu, E., Kozu, M., Koga, K., Lee, A., Matsuhara, H., Mima, S., Mitsuda, K., Mizukami, K., Morii, H., Morishima, T., Nagai, M., Nagata, R., Nakamura, S., Naruse, M., Namikawa, T., Natsume, K., Nishibori, T., Nishijo, K., Nishino, H., Noda, A., Noguchi, T., Ogawa, H., Oguri, S., Ohta, I. S., Okada, N., Otani, C., Richards, P., Sakai, S., Sato, N., Sato, Y., Segawa, Y., Sekimoto, Y., Shinozaki, K., Sugita, H., Suzuki, A., Suzuki, T., Tajima, O., Takada, S., Takakura, S., Takei, Y., Tomaru, T., Uzawa, Y., Wada, T., Watanabe, H., Yamada, Y., Yamaguchi, H., Yamasaki, N., Yoshida, M., Yoshida, T., and Yotsumoto, K., "LiteBIRD: mission overview and design tradeoffs," in [*SPIE Astronomical Telescopes + Instrumentation*], Oschmann, J. M., Clampin, M., Fazio, G. G., and MacEwen, H. A., eds., 91431F, International Society for Optics and Photonics (aug 2014).
- [3] Matsumura, T., Akiba, Y., Arnold, K., Borrill, J., Chendra, R., Chinone, Y., Cukierman, A., de Haan, T., Dobbs, M., Dominjon, A., Elleflot, T., Errard, J., Fujino, T., Fuke, H., Goeckner-wald, N., Halverson, N., Harvey, P., Hasegawa, M., Hattori, K., Hattori, M., Hazumi, M., Hill, C., Hilton, G., Holzapfel, W., Hori, Y., Hubmayr, J., Ichiki, K., Inatani, J., Inoue, M., Inoue, Y., Irie, F., Irwin, K., Ishino, H., Ishitsuka, H., Jeong, O., Karatsu, K., Kashima, S., Katayama, N., Kawano, I., Keating, B., Kibayashi, A., Kibe, Y.,

Kida, Y., Kimura, K., Kimura, N., Kohri, K., Komatsu, E., Kuo, C. L., Kuromiya, S., Kusaka, A., Lee, A., Linder, E., Matsuhara, H., Matsuoka, S., Matsuura, S., Mima, S., Mitsuda, K., Mizukami, K., Morii, H., Morishima, T., Nagai, M., Nagasaki, T., Nagata, R., Nakajima, M., Nakamura, S., Namikawa, T., Naruse, M., Natsume, K., Nishibori, T., Nishijo, K., Nishino, H., Nitta, T., Noda, A., Noguchi, T., Ogawa, H., Oguri, S., Ohta, I. S., Otani, C., Okada, N., Okamoto, A., Okamura, T., Rebeiz, G., Richards, P., Sakai, S., Sato, N., Sato, Y., Segawa, Y., Sekiguchi, S., Sekimoto, Y., Sekine, M., Seljak, U., Sherwin, B., Shinozaki, K., Shu, S., Stompor, R., Sugai, H., Sugita, H., Suzuki, T., Suzuki, A., Tajima, O., Takada, S., Takakura, S., Takano, K., Takei, Y., Tomaru, T., Tomita, N., Turin, P., Utsunomiya, S., Uzawa, Y., Wada, T., Watanabe, H., Westbrook, B., Whitehorn, N., Yamada, Y., Yamasaki, N., Yamashita, T., Yoshida, M., Yoshida, T., and Yotsumoto, Y., “LiteBIRD: Mission Overview and Focal Plane Layout,” *Journal of Low Temperature Physics* (2016).

- [4] Ishino, H., Akiba, Y., Arnold, K., Barron, D., Borrill, J., Chandra, R., Chinone, Y., Cho, S., Cukierman, A., de Haan, T., Dobbs, M., Dominjon, A., Dotani, T., Elleflot, T., Errard, J., Fujino, T., Fuke, H., Funaki, T., Goeckner-Wald, N., Halverson, N., Harvey, P., Hasebe, T., Hasegawa, M., Hattori, K., Hattori, M., Hazumi, M., Hidehira, N., Hill, C., Hilton, G., Holzzapfel, W., Hori, Y., Hubmayr, J., Ichiki, K., Imada, H., Inatani, J., Inoue, M., Inoue, Y., Irie, F., Irwin, K., Ishitsuka, H., Jeong, O., Kanai, H., Karatsu, K., Kashima, S., Katayama, N., Kawano, I., Kawasaki, T., Keating, B., Kernasovskiy, S., Keskitalo, R., Kibayashi, A., Kida, Y., Kimura, N., Kimura, K., Kisner, T., Kohri, K., Komatsu, E., Komatsu, K., Kuo, C.-L., Kuromiya, S., Kusaka, A., Lee, A., Li, D., Linder, E., Maki, M., Matsuhara, H., Matsumura, T., Matsuoka, S., Matsuura, S., Mima, S., Minami, Y., Mitsuda, K., Nagai, M., Nagasaki, T., Nagata, R., Nakajima, M., Nakamura, S., Namikawa, T., Naruse, M., Nishibori, T., Nishijo, K., Nishino, H., Noda, A., Noguchi, T., Ogawa, H., Ogburn, W., Oguri, S., Ohta, I., Okada, N., Okamoto, A., Okamura, T., Otani, C., Pisano, G., Rebeiz, G., Richards, P., Sakai, S., Sakurai, Y., Sato, Y., Sato, N., Segawa, Y., Sekiguchi, S., Sekimoto, Y., Sekine, M., Seljak, U., Sherwin, B., Shimizu, T., Shinozaki, K., Shu, S., Stompor, R., Sugai, H., Sugita, H., Suzuki, J., Suzuki, T., Suzuki, A., Tajima, O., Takada, S., Takakura, S., Takano, K., Takatori, S., Takei, Y., Tanabe, D., Tomaru, T., Tomita, N., Turin, P., Uozumi, S., Utsunomiya, S., Uzawa, Y., Wada, T., Watanabe, H., Westbrook, B., Whitehorn, N., Yamada, Y., Yamamoto, R., Yamasaki, N., Yamashita, T., Yoshida, T., Yoshida, M., and Yotsumoto, K., “Litebird: lite satellite for the study of B-mode polarization and inflation from cosmic microwave background radiation detection,” in [*Proc. SPIE*], **9904**, 99040X–99040X–8 (2016).
- [5] Hazumi, M. et al., “Litebird: A satellite for the studies of b-mode polarization and inflation from cosmic background radiation detection,” *J. of Low Temperature Physics* **xxx**, in press (2018).
- [6] Seljak, U. b. u. and Zaldarriaga, M., “Signature of gravity waves in the polarization of the microwave background,” *Phys. Rev. Lett.* **78**, 2054–2057 (Mar 1997).
- [7] Kamionkowski, M., Stebbins, A., Kosowsky, A., and Stebbins, A., “A Probe of Primordial Gravity Waves and Vorticity,” *Phys. Rev. Lett.* **78**, 2058–2061 (mar 1997).
- [8] Zaldarriaga, M. and Seljak, U., “All-sky analysis of polarization in the microwave background,” *Phys. Rev. D* **55**(4), 1830–1840 (1997).
- [9] Kamionkowski, M., Kosowsky, A., and Stebbins, A., “Statistics of cosmic microwave background polarization,” *Phys. Rev. D* **55**(12), 7368–7388 (1997).
- [10] Kamionkowski, M. and Kovetz, E. D., “The Quest for B Modes from Inflationary Gravitational Waves,” *Annu. Rev. Astron. Astrophys.* **54**, 227–69 (oct 2016).
- [11] Ade, P. A. R., Ahmed, Z., Aikin, R. W., Alexander, K. D., Barkats, D., Benton, S. J., Bischoff, C. A., Bock, J. J., Bowens-Rubin, R., Brevik, J. A., Buder, I., Bullock, E., Buza, V., Connors, J., Crill, B. P., Duband, L., Dvorkin, C., Filippini, J. P., Fliescher, S., Grayson, J., Halpern, M., Harrison, S., Hilton, G. C., Hui, H., Irwin, K. D., Karkare, K. S., Karpel, E., Kaufman, J. P., Keating, B. G., Kefeli, S., Kernasovskiy, S. A., Kovac, J. M., Kuo, C. L., Leitch, E. M., Lueker, M., Megerian, K. G., Netterfield, C. B., Nguyen, H. T., O’Brien, R., Ogburn, R. W., Orlando, A., Pryke, C., Richter, S., Schwarz, R., Sheehy, C. D., Staniszewski, Z. K., Steinbach, B., Sudiwala, R. V., Teply, G. P., Thompson, K. L., Tolan, J. E., Tucker, C., Turner, A. D., Vieregg, A. G., Weber, A. C., Wiebe, D. V., Willmert, J., Wong, C. L., Wu, W. L. K., and Yoon, K. W., “Improved Constraints on Cosmology and Foregrounds from BICEP2 and Keck Array Cosmic Microwave Background Data with Inclusion of 95 GHz Band,” *Physical Review Letters* **116**(3) (2016).

- [12] Hasebe, T. et al., “Thermal design utilizing radiative cooling for the payload module of LiteBIRD,” in [*Proc. SPIE*], **10698**, xxx (2018).
- [13] Tsujimoto, M. et al., “Electrical system design of the payload of LiteBIRD,” in [*Proc. SPIE*], **10698**, xxx (2018).
- [14] Suzuki, A. et al., “The litebird satellite mission - sub-kelvin instrument,” *J. of Low Temperature Physics* **xxx**, in press (2018).
- [15] Imada, H. et al., “The optical design and physical optics analysis of a cross-Dragonian telescope for LiteBIRD,” in [*Proc. SPIE*], **10698**, xxx (2018).
- [16] Sakurai, Y., Matsumura, T., Iida, T., Kanai, H., Katayama, N., Imada, H., Ohsaki, H., Terao, Y., Shimomura, T., Sugai, H., Kataza, H., Yamamoto, R., and Utsunomiya, S., “Design and thermal characteristics of a 400 mm diameter levitating rotor in a superconducting magnetic bearing operating below at 10 k for a cmb polarization experiment,” *IEEE Transactions on Applied Superconductivity* **28**, 1–4 (June 2018).
- [17] Errard, J., Feeney, S. M., Peiris, H. V., and Jaffe, A. H., “Robust forecasts on fundamental physics from the foreground-obscured, gravitationally-lensed CMB polarization,” *Journal of Cosmology and Astroparticle Physics* **3**, 052 (Mar. 2016).
- [18] Stompor, R., Errard, J., and Poletti, D., “Forecasting performance of CMB experiments in the presence of complex foreground contaminations,” *Phys. Rev. D* **94**(8), 83526 (2016).
- [19] Remazeilles, M., Dickinson, C., Eriksen, H. K., and Wehus, I. K., “Joint Bayesian estimation of tensor and lensing B modes in the power spectrum of CMB polarization data,” *Monthly Notices of the Royal Astronomical Society* **474**, 3889–3897 (Mar. 2018).
- [20] Ichiki, K., “CMB foreground: A concise review,” *Progress of Theoretical and Experimental Physics* **2014** (jun 2014).
- [21] Katayama, N. and Komatsu, E., “Simple Foreground Cleaning Algorithm for Detecting Primordial B-mode Polarization of the Cosmic Microwave Background,” *The Astrophysical Journal* **737**(2), 78 (2011).
- [22] Hoang, D. T., Patanchon, G., Bucher, M., Matsumura, T., Banerji, R., Ishino, H., Hazumi, M., and Delabrouille, J., “Bandpass mismatch error for satellite cmb experiments i: estimating the spurious signal,” *Journal of Cosmology and Astroparticle Physics* **2017**(12), 015 (2017).
- [23] Essinger-Hileman, T., Kusaka, A., Appel, J. W., Choi, S. K., Crowley, K., Ho, S. P., Jarosik, N., Page, L. A., Parker, L. P., Raghunathan, S., Simon, S. M., Staggs, S. T., and Visnjic, K., “Systematic effects from an ambient-temperature, continuously rotating half-wave plate,” *Review of Scientific Instruments* **87**, 094503 (sep 2016).
- [24] Sugai, H., Kashima, S., Kimura, K., Matsumura, T., Inoue, M., Ito, M., Nishibori, T., Sekimoto, Y., Ishino, H., Sakurai, Y., Imada, H., and Fujii, T., “Optical designing of LiteBIRD,” in [*Proc. SPIE*], **9904**, 99044H–99044H–7 (2016).
- [25] Pisano, G., Maffei, B., Ade, P. A. R., de Bernardis, P., de Maagt, P., Ellison, B., Henry, M., Ng, M. W., Schortt, B., and Tucker, C., “Multi-octave metamaterial reflective half-wave plate for millimeter and sub-millimeter wave applications,” *Appl. Opt.* **55**(36), 10255–10262 (2016).
- [26] Hasebe, T. et al., “Concept study of optical configurations for high frequency telescope for litebird,” *J. of Low Temperature Physics* **24**, in press (2018).
- [27] Bernacki, B. E., Kelly, J. F., Sheen, D., Hatchell, B., Valdez, P., Tedeschi, J., Hall, T., and McMakin, D., “Wide-field-of-view millimeter-wave telescope design with ultra-low cross-polarization,” in [*SPIE*], **8362**, 836207–836211 (may 2012).
- [28] Kashima, S. et al., “Wide field-of-view crossed dragone optical system using anamorphic aspherical surfaces,” *Applied optics* **57**, in press (2018).
- [29] Tran, H., Johnson, B., Dragovan, M., Bock, J., Aljabri, A., Amblard, A., Bauman, D., Betoule, M., Chui, T., Colombo, L., Cooray, A., Crumb, D., Day, P., Dickenson, C., Dowell, D., Golwala, S., Gorski, K., Hanany, S., Holmes, W., Irwin, K., Keating, B., Kuo, C.-L., Lee, A., Lange, A., Lawrence, C., Meyer, S., Miller, N., Nguyen, H., Pierpaoli, E., Ponthieu, N., Puget, J.-L., Raab, J., Richards, P., Satter, C., Seiffert, M., Shimon, M., Williams, B., and Zmuidzinas, J., “Optical Design of the EPIC-IM Crossed Dragone Telescope,” in [*SPIE*], Atad-Ettedgui, E. and Lemke, D., eds., **7731**, 77311R–77311R–15 (jul 2010).

- [30] Rodriguez, J., Geise, A., Schmidt, C. H., Migl, J., and Steiner, H. J., “Asymptotic and full wave simulation models for compensated compact range design and analysis,” in [2013 Loughborough Antennas Propagation Conference (LAPC)], 461–466 (Nov 2013).
- [31] “TICRA.” <http://www.ticra.com/software/grasp/>.
- [32] Tauber, J. A., Norgaard-Nielsen, H. U., Ade, P. A. R., Amiri Parian, J., Banos, T., Bersanelli, M., Burigana, C., Chamballu, A., de Chambure, D., Christensen, P. R., Corre, O., Cozzani, A., Crill, B., Crone, G., D’Arcangelo, O., Daddato, R., Doyle, D., Dubruel, D., Forma, G., Hills, R., Huffenberger, K., Jaffe, A. H., Jessen, N., Kletzkine, P., Lamarre, J. M., Leahy, J. P., Longval, Y., de Maagt, P., Maffei, B., Mandolesi, N., Martí-Canales, J., Martín-Polegre, A., Martin, P., Mendes, L., Murphy, J. A., Nielsen, P., Noviello, F., Paquay, M., Peacocke, T., Ponthieu, N., Pontoppidan, K., Ristorcelli, I., Riti, J.-B., Rolo, L., Rosset, C., Sandri, M., Savini, G., Sudiwala, R., Tristram, M., Valenziano, L., van der Vorst, M., van ’t Klooster, K., Villa, F., and Yurchenko, V., “Planck pre-launch status: The optical system,” *A&A* **520**, A2 (2010).
- [33] Sakurai, Y. et al., “Design and development of a polarization modulator unit based on a continuous rotating half-wave plate for LiteBIRD,” in [Proc. SPIE], **10708**, xxx (2018).
- [34] “TK-RAM.” <http://www.terahertz.co.uk/>.
- [35] Saily, J. and Raisanen, A., “Characterization of Submillimeter Wave Absorbers from 200 - 600 GHz,” *International Journal of Infrared and Millimeter Waves* **5**, 71 (2004).
- [36] “NASA outgassing data.” <https://outgassing.nasa.gov/cgi/uncgi/search/search.html.sh>.
- [37] Edwards, J. M., O’Brien, R., Lee, A. T., and Rebeiz, G. M., “Dual-Polarized Sinuous Antennas on Extended Hemispherical Silicon Lenses,” *IEEE Transactions on Antennas and Propagation* **60**, 4082–4091 (sep 2012).
- [38] Beckman, S. et al., “Development of cosmic ray mitigation techniques for the LiteBIRD space mission,” in [Proc. SPIE], **10708**, xxx (2018).
- [39] Ade, P. A. R., Pisano, G., Tucker, C., and Weaver, S., “A review of metal mesh filters,” in [SPIE], 62750U–62750U (2006).
- [40] Ogawa, H., Nakagawa, T., Matsuhara, H., Shinozaki, K., Goto, K., Isobe, N., Kawada, M., Mizutani, T., Sato, Y., Sugita, H., Takeuchi, S., Yamawaki, T., and Shibai, H., “New cryogenic system of the next-generation infrared astronomy mission SPICA,” in [Proc. SPIE], **9904**, 99042H–10 (2016).
- [41] Shinozaki, K., Ogawa, H., Nakagawa, T., Sato, Y., Sugita, H., Yamawaki, T., Mizutani, T., Matsuhara, H., Kawada, M., Okabayashi, A., Tsunematsu, S., Narasaki, K., and Shibai, H., “Mechanical cooler system for the next-generation infrared space telescope SPICA,” in [Proc. SPIE], **9904**, 99043W–8 (2016).
- [42] Bard, S., Stein, J., and Petrick, W., “Advanced radiative cooler with angled shields,” *Progress in Astronautics and Aeronautics* **83**, 249 – 258 (1982).
- [43] Planck Collaboration, “Planck early results. II. The thermal performance of Planck,” *Astronomy & Astrophysics* **536**, A2 (2011).
- [44] Duval, J.-M., Duband, L., and Attard, A., “Qualification campaign of the 50 mk hybrid sorption-adr cooler for spica/safari,” *IOP Conference Series: Materials Science and Engineering* **101**(1), 012010 (2015).
- [45] Prouvé, T., Duval, J. M., Charles, I., Yamasaki, N. Y., Mitsuda, K., Nakagawa, T., Shinozaki, K., Tokoku, C., Yamamoto, R., Minami, Y., Du, M. L., Andre, J., Daniel, C., and Linder, M., “ATHENA X-IFU 300 K-50 mK cryochain demonstrator cryostat,” *Cryogenics* **89**(July 2017), 85–94 (2018).
- [46] Chaudhry, G., Volpe, A., Camus, P., Triqueneaux, S., and Vermeulen, G., “A closed-cycle dilution refrigerator for space applications,” *Cryogenics* **52**(10), 471 – 477 (2012).
- [47] Takahashi, T. et al., “Hitomi (astro-h) x-ray astronomy satellite,” *Journal of Astronomical Telescopes, Instruments, and Systems* **4**, 4 – 4 – 13 (2018).
- [48] Manabe, T., Nishibori, T., Mizukoshi, K., Otsubo, F., Ochiai, S., and Ohmine, H., “Measurement of the Offset-Cassegrain Antenna of JEM/SMILES Using a Near-Field Phase-Retrieval Method in the 640-GHz Band,” *IEEE Transactions on Antennas and Propagation* **60**(8), 3971–3976 (2012).
- [49] Hirata, A., Nagatsuma, T., Yano, R., Ito, H., Furuta, T., Hirota, Y., Ishibashi, T., Matsuo, H., Ueda, A., Noguchi, T., Sekimoto, Y., Ishiguro, M., and Matsuura, S., “Output power measurement of photonic millimeter-wave and sub-millimeter-wave emitter at 100-800 GHz,” *Electron Lett* **38**, 798 (2002).
- [50] Kiuchi, H., Kawanishi, T., and Kanno, A., “Wide frequency range optical synthesizer with high-frequency resolution,” *IEEE Photonics Technology Letters* **29**, 78–81 (Jan 2017).